ELSEVIER

Journal of Quantitative Spectroscopy & Radiative Transfer 109 (2008) 151–167

Journal of Quantitative Spectroscopy & Radiative Transfer

www.elsevier.com/locate/jqsrt

Laser spectroscopic monitoring of gas emission and measurements of the $^{13}C/^{12}C$ isotope ratio in CO_2 from a wood-based combustion

Julien Cousin[a], Weidong Chen[a,*], Marc Fourmentin[a], Eric Fertein[a], Daniel Boucher[a], Fabrice Cazier[b], Habiba Nouali[b], Dorothée Dewaele[b], Marc Douay[c], Laurence S. Rothman[d]

[a]*Laboratoire de PhysicoChimie de l'Atmosphère, CNRS UMR 8101, Université du Littoral Côte d'Opale, 189 A Av. Maurice Schumann, 59140 Dunkerque, France*

[b]*Centre Commun de Mesures, Université du Littoral Côte d'Opale 145 Av. Maurice Schumann, 59140 Dunkerque, France*

[c]*Laboratoire de Physique des Lasers, Atomes et Molécules, CNRS UMR 8523, Université des Sciences et Technologies de Lille, 59655 Villeneuve d'Ascq Cedex, France*

[d]*Harvard-Smithsonian Center for Astrophysics, Atomic and Molecular Physics Division MS50, 60 Garden Street, Cambridge, MA 02138-1516, USA*

Received 13 November 2006; received in revised form 27 May 2007; accepted 29 May 2007

Abstract

We report on the application of a compact and field-deployable instrument, based on a continuous-wave fiber-coupled Telecom external cavity diode laser, to measure the $^{13}C/^{12}C$ isotope ratio in CO_2 from a wood-based combustion. Carbon dioxide, the most important greenhouse gas, is a major product of combustion. The measurements of the $^{13}C/^{12}C$ isotopic ratio in CO_2 from combustion emission permit one to identify the CO_2 source and to study the temporal and spatial variations of pollution in the atmosphere. The average value of the $^{13}CO_2/^{12}CO_2$ ratio is found to be $(1.1011 \pm 0.0024)\%$. The corresponding δ-value relative to PDB standard is $(-20.17 \pm 2.14)‰$, which is in good agreement with the typical value of $(-25 \pm 2)‰$ for wood. Simultaneous monitoring of multiple species from gas emission has been performed using direct-absorption spectroscopy. The concentrations of C_2H_2, CO, CO_2 and H_2O were determined on the basis of integrated absorbance measured by least-squares fitting a Voigt lineshape to experimental absorption spectra.

Keywords: Near-infrared spectroscopy; $^{13}CO_2/^{12}CO_2$ isotopic ratio; Combustion gases measurements; External cavity diode laser

1. Introduction

During the last decade, the need for optical telecommunication has spurred the development of continuous-wave tunable lasers in the near infrared around 1.55 μm. Today, these devices are finding an increasing

*Corresponding author. Tel.: +33 3 2865 8264; fax: +33 3 2865 8244.
E-mail address: chen@univ-littoral.fr (W. Chen).

0022-4073/$ - see front matter © 2007 Elsevier Ltd. All rights reserved.
doi:10.1016/j.jqsrt.2007.05.010

number of applications not only in the telecommunication domain, but also in high-resolution molecular spectroscopy and ultra-sensitive spectroscopic detection of trace gases in various areas, e.g. environmental and climate research, industry, agriculture, homeland security and medical diagnosis.

In this paper, we report on the application of a compact and field-deployable instrument for measuring the $^{13}CO_2/^{12}CO_2$ isotope ratio and monitoring gas emission from a wood-based combustion. Carbon dioxide is a major product of combustion. The measurements of the $^{13}CO_2/^{12}CO_2$ isotopic ratio allow for the identification of the CO_2 source and for the study of the temporal and spatial variations of pollution in the atmosphere.

Laser absorption spectroscopy was first applied to CO_2 isotopes measurement in the early 1990s by Becker et al. [1] and Murnick et al. [2]. Recently, measurements of $^{13}CO_2/^{12}CO_2$ isotopic ratio in a calibrated CO_2/N_2 mixture by infrared laser absorption spectroscopy have been reported by Erdélyi et al. [3] using a laser difference frequency-based sensor at 4.35 μm, by Gagliardi, Castrillo et al. using a DFB laser operating at 2008 nm [4,5], by Weidmann et al. [6] using a quantum cascade laser at 4.32 μm. Real-world applications have been reported by McManus et al. [7] in human breath, ambient air and automobile exhaust, by Castrillo et al. [8] in volcanic emission, by Crosson et al. [9] and Kasyutich et al. [10] in human breath.

Tunable diode laser-based measurements of combustion gases have been recently reported by a number of groups. For instance, measurements in combustion environments have been carried out for the following species: NO in a H_2–air flame [11]; CO, CO_2 and CH_4 in combustion gases from a CH_4–air flat-flame burner [12]; CO, CO_2, OH and H_2O in the exhaust gases of a CH_4–air flame [13]; OH radical in the postflame region of a two-dimensional laminar counterflow burner [14]; CO in a C_2H_4–air flame [15]; CO_2 from a C_2H_4–air flat-flame burner [16]; CO and H_2O in the exhaust-gas region above a laboratory burner fueled with CH_4 and C_3H_6 [17] and in a full-sized coal-fired power plant [18].

In the present work, a continuous-wave fiber-coupled Telecom external cavity diode laser broadly tunable from 1500 to 1640 nm was used for simultaneous measurements of the $^{13}CO_2/^{12}CO_2$ isotope ratio and C_2H_2, CO, CO_2, H_2O concentrations in wood-fired combustion gases. The spectroscopic measurements have been performed based on integrated absorbance determination by least-squares fitting a Voigt lineshape to experimental absorption spectra.

2. Instrumental set-up

The experimental set-up, mounted on a $60 \times 60\,cm^2$ optical breadboard, is depicted in Fig. 1. It is based on a fiber-coupled Telecom external cavity diode laser (ECDL, Tunics Plus) emitting single-mode and single-frequency radiation with an output optical power up to 5 mW. This laser source is mode-hop free continuously

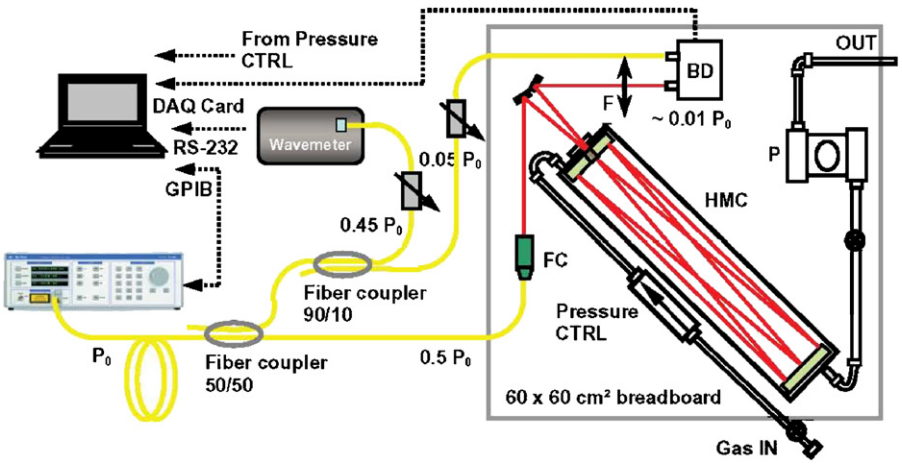

Fig. 1. Experimental set-up of a fiber-coupled ECDL spectrometer developed in the present work. FC: fiber connector; HMC: Herriott multipass cell; P: two-stage diaphragm pump; BD: balanced detector; pressure CTRL: pressure controller.

tunable in the near infrared from 1500 to 1640 nm (C and L band) with a tuning resolution of 0.001 nm ($-4\times10^{-3}\,\mathrm{cm}^{-1}$). The laser emission linewidth, determined by heterodyne measurements in the present work, is less than 1 MHz. The laser output power was split off by a 50/50 fiber coupler into two parts. One was coupled to a fiber pigtailed collimator using a GRIN (GRadient INdex) lens ($f=4.7$ mm), which formed a collimated beam of 1 mm in diameter, and then the collimated beam was directed to a multipass cell in Herriott configuration. The multipass cell, equipped with a wedged entrance window, has a fixed optical path of 100 m and a volume of 3.2 L (New Focus, Model 5612). A two-stage oil-free diaphragm pump (KNF Neuberger) was used to evacuate the cell and provide a flow up to 5 N L/min for continuous measurement application. The gas pressure inside the cell was measured and controlled by a pressure controller (MKS 640). The emerging absorption signal from the cell was focused onto an InGaAs-balanced photodiode detector (New Focus, Model Nirvana 2007). The remaining laser emission fraction was divided again into two parts with a 90/10 fiber coupler: the main part was fiber coupled to a wavemeter (Burleigh, Model WA-1500) for wavelength measurements with a resolution of 10^{-4} nm and a relative accuracy of about $\pm10^{-7}$, and the other, used as reference signal, was fiber coupled to the balanced photodiode detector. Optical power received by the wavemeter and the reference channel of the balanced detector could be adjusted by using a variable fiber attenuator (0–40 dB), respectively.

The measured wavelength values were sent to a personal computer via a serial communication port (RS-232). Wavelength scan of the ECDL was controlled by a Labview-based program through a general-purpose interface bus (GPIB) communication interface (National Instruments, GPIB-USB-B). Data acquisition of absorption signal was performed by using a National Instruments acquisition card (DAQ card, Model PCI-MIO16E1) with a sampling rate up to 1.2 MS/s. Spectroscopic absorption signal and wavelength were simultaneously recorded. In order to improve the signal-to-noise ratio (SNR), the spectral signal at each wavelength was averaged during the laser wavelength scan. This is in contrast to conventional "sweep integration" technique [19], where the wavelength is repeatedly swept over absorption line(s) and the absorption spectrum recorded on each sweep is averaged. The technique involving signal average "point by point" is usually employed for laser wavelength tuning by temperature [20,21]. This averaging method eliminates the effect of low-frequency spectral drift of the diode laser on the averaged spectra [22], and permits us to measure precisely the wavelength for each sampling data as the used wavemeter offers a measurement rate of 1 Hz. Operation of the laser instrument (wavelength scan and data acquisition) was controlled and monitored with a LabView-based software developed in the laboratory. The overall system can be used for field operation in a fully automated mode, 24 h per day and 7 days per week, without operator intervention.

3. Instrumental characterization

3.1. Concentration measurements of gas species

Laser-based spectroscopic analysis of trace gas concentration is based on measurements of frequency-dependent absorption of molecules over a given optical path length. The measurement of a specific molecular absorption spectrum allows the identification and quantification of gas species based on the Beer–Lambert law. Gas concentration can be retrieved either by fitting a characteristic spectral absorption profile to a theoretical model using molecular line parameters, or by using a validated calibration standard.

Based upon the Beer–Lambert law, the absorbance, $A(\nu)$, at frequency ν can be expressed as

$$A(\nu)=\ln(I_0/I(\nu))=N\sigma(\nu)L, \tag{1}$$

where $I(\nu)$ and I_0 are the transmitted and incident light power, respectively; N is the number of absorbing molecules per cubic centimeter in molecules/cm^3; $\sigma(\nu)$ is the frequency-dependent absorption cross section in cm^2/mol and L is the optical absorption path length in cm. The integrated absorbance, A_I in cm^{-1} can be written as

$$A_\mathrm{I}=\int A(\nu)\,\mathrm{d}\nu=\int \ln(I_0/I(\nu))\,\mathrm{d}\nu=NL\int\sigma(\nu)\,\mathrm{d}\nu=NLS \tag{2}$$

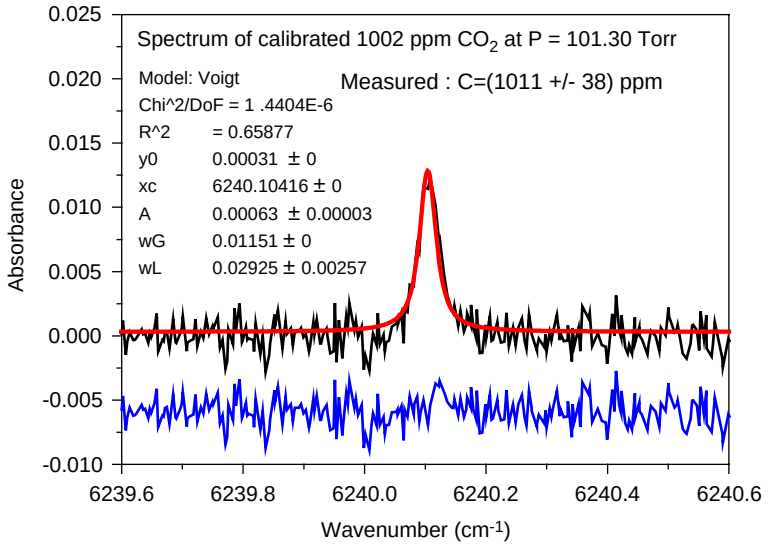

Fig. 2. Concentration measurement: black curve, absorption spectrum of 1002 ppm CO_2 at $P = 101.3$ Torr; red curve, Voigt model-based spectroscopic lineshape fit; blue line, fit residual. Parameters of the Voigt fit: χ^2, the chi-square parameter and R^2, the fit correlation coefficient; $y0$ = offset; xc = peak center position; A = integrated area under the absorption line profile; wG = Gaussian width; wL = Lorentzian width.

with $S = \int \sigma(v)\,dv$, the molecule absorption line intensity in $cm^{-1}/(mol\,cm^{-2})$. In this way, the concentration of the absorbing molecules in ppm (part per million) can be determined by

$$C(\text{ppm}) = \frac{N}{N_T} \times 10^6 = \frac{A_I P_0 T}{N_L P T_0 L S} \times 10^6, \tag{3}$$

where $N_L = 2.6868 \times 10^{19}\,mol/cm^3$ is the Loschmidt number at $T_0 = 273.15\,K$ and $P_0 = 760\,Torr$.

The dependence of the absorption line intensity on the temperature T can be described as follows [23]:

$$\frac{S_{lu}(T)}{S_{lu}(T_{ref})} = \frac{Q(T_{ref})}{Q(T)} \frac{[1-\exp(-c_2 v_{lu}/T)]}{[1-\exp(-c_2 v_{lu}/T_{ref})]} \frac{\exp(-c_2 E_l/T)}{\exp(-c_2 E_l/T_{ref})}, \tag{4}$$

where $T_{ref} = 296\,K$, and v_{lu} is the frequency (cm^{-1}) of the line transition between lower and upper states l and u. S_{lu} is the spectral line intensity ($cm^{-1}/(mol\,cm^{-2})$), and c_2 the second radiation constant $= hc/k = 1.4388\,cm\,K$ with h, c and k being the Planck constant, the speed of light (in vacuum) and the Boltzmann constant, respectively. Q is the total internal partition sum and E_l is the lower state energy (cm^{-1}). The ratio of total internal partition functions for linear molecules like CO_2, CO and C_2H_2 can be approximately calculated using the parameterization given in Ref. [24] and the relation for H_2O is given in Ref. [25].

For calibration and validation purposes, a calibrated mixture standard was used. Concentration measurements of CO_2 with a specified mixing ratio of 1002 ± 20 ppm were carried out. In Fig. 2, the black curve corresponds to absorption spectrum of 1002 ppm CO_2 from a standard cylinder, and the red curve is the Voigt model-based spectral lineshape fit. Based on Eq. (3) by using the line parameters given in the HITRAN database [23], a concentration of 1011 ppm was retrieved from the integrated area under the absorption peak. This value is in good agreement with the gas mixture specification within the estimated $\pm 3.7\%$ measurement uncertainty. The relative accuracy of 0.9%, which represents the relative deviation of the measured value from the value given by the standard-gas mixture, is mainly limited by the uncertainties on L, P, T and S (see Eq. (3)) used for concentration retrieval.

3.2. Dynamic measurement range

One of the most important specific parameters for an analytical instrument is the measurement dynamics that is usually limited by the linear response range of the detector. In spectroscopic absorption-based

concentration measurements, high dynamic range detection using a single detector may be realized by using strong and weak absorption lines for low and high concentration measurements, respectively. In order to ensure the linearity of the spectrometer, the used absorption lines have to be selected so that the line intensities allow the spectrometer to scale linearly with the absorption intensity that is proportional to the measured gas concentration. In the present work, the spectrometer linearity has been checked for each absorption line involved for low or high concentration measurements.

The dynamic measurement range of the developed laser instrument has been evaluated with measurements of C_2H_2 at different mixing ratios. By selecting a strong or weak transition line available in the spectral coverage of the laser source, highly dynamic detection of gas concentration ranging from 100% purity to sub-ppm level can be achieved using the same instrument. Fig. 3 shows two absorption spectra of C_2H_2, recorded

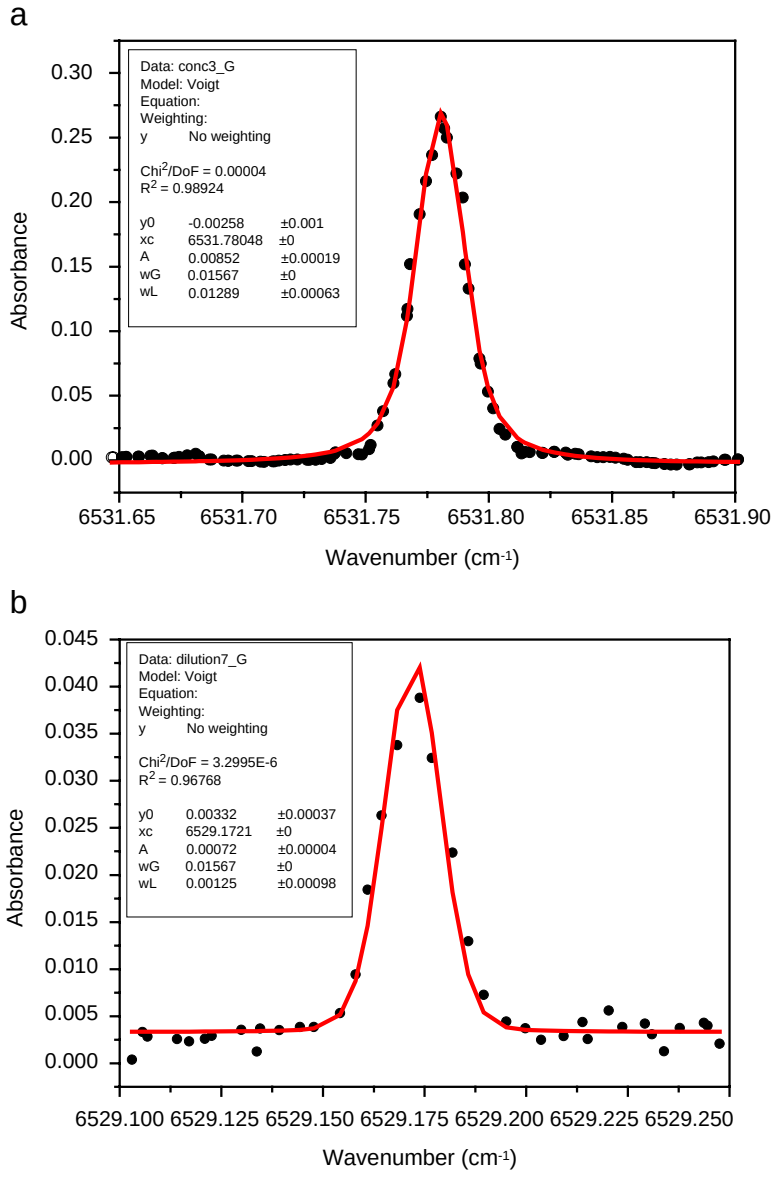

Fig. 3. Measurements of C_2H_2 at different concentration levels: (a) high concentration (500 ppm) absorption spectrum around 6531.7805 cm^{-1} and (b) trace level (18.9 ppm) absorption spectrum near 6529.1721 cm^{-1}. The used absorption lines correspond to the following transitions lines: $P_e(10)$ and $P_e(11)$ of the $\nu_1+\nu_3(\Sigma_u^+)$–$0(\Sigma_g^+)$ combination band with line intensities at 296 K of 4.00×10^{-21} and 1.17×10^{-20} $cm^{-1}/(molecule\times cm^{-2})$, respectively.

at 10 mbar: (a) at high concentration (500 ppm) around 6531.7805 cm^{-1} and (b) at trace level (18.9 ppm) at 6529.1721 cm^{-1}. Ambient air was used to dilute the C_2H_2 sample. The used absorption lines were assigned to the following transitions lines [23]: $P_e(10)$ and $P_e(11)$ of the $v_1+v_3(\Sigma_u^+)$–$0(\Sigma_g^+)$ combination band with line intensities (at 296 K) of 4.00×10^{-21} and 1.17×10^{-20} $cm^{-1}/(mol\,cm^{-2})$, respectively. Higher concentration of several percents up to 100% could be measurable by the present set-up using the transition line $R_f(1)$ of the $v_1+v_3+v_4^1(\Pi_u)$–$v_4^1(\Pi_g)$ hot band near 6534.457 cm^{-1} whose line intensity is 5.06×10^{-23} $cm^{-1}/(mol\,cm^{-2})$.

3.3. Measurement sensitivity

Another important parameter to be characterized is the measurement sensitivity, usually expressed in terms of the minimum detectable absorption coefficient. A long optical path length absorption approach was used to enhance the absorption signal by means of a multipass cell based on multiple reflections. In this long optical path length absorption approach, trace gas detection is based on the measurement of absorption signal as a small change in the total transmitted probing source intensity. The detection sensitivity and thus the precision of spectroscopic analysis are usually limited by fluctuations in the probing laser source and optical interference fringes arising from the multiple pass cell. In the present work, reduction of the laser intensity noise was achieved by averaging the spectral signal at each wavelength during the wavelength scan. In order to determine the optimal average number N_{av}, the Allan variance study [26–28] has been carried out. For this study, direct absorption spectra of CO_2 near 6254 cm^{-1} with constant concentration have been repetitively recorded as the data average number is successively increased. A nonlinear least-squares fit (NLSF) method was used to determine CO_2 absorbance by fitting the absorption spectra to a Voigt lineshape model. The standard deviation of the determined absorbance is converted to $1-\sigma$ minimum detectable absorption coefficient and is plotted in Fig. 4 (blue dots) as a function of the data average number N_{av} that is proportional to the integration time. The standard deviation, theoretically predicted to be inversely proportional to $(N_{av})^{1/2}$, is also shown in the figure (red curve). As can be seen, the measurement sensitivity increases at first with integration time (average number). After an optimum value is reached, the instabilities of the instrumental system may counterbalance the noise reduction given by average. The χ^2-square parameter resulted from

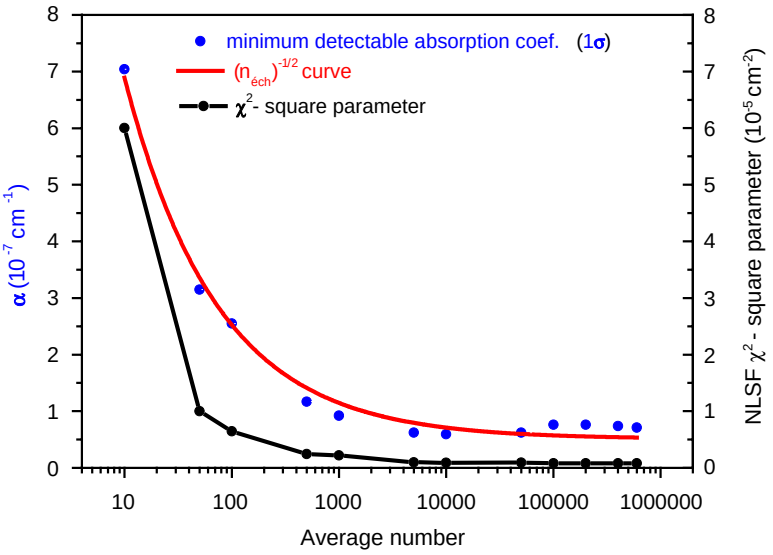

Fig. 4. Evolution of the standard deviation of the determined absorbance with the average number N_{av} per sampling wavelength datum, where the standard deviation is converted to $1-\sigma$ minimum detectable absorption coefficient (blue dots), σ represents the standard deviation associated with a set of repeated measurements. The standard deviation is proportional to $(N_{av})^{-1/2}$ (red curve), as theoretically predicted. The χ^2-square parameter resulted from nonlinear least squares fit (NLSF) that characterizes the fit quality is also shown (black dots). According to the Allan variance analysis, the optimum co-adds number was 600 000.

NLSF that characterizes the fit quality is also shown in Fig. 4 (black dots), which confirms the Allan variance analysis result mentioned above.

As gas mixture concentrations are retrieved from the integrated absorbances determined by a Voigt fit to the experimental absorption profiles, the relative uncertainty in the estimation of the integrated areas is determined by the SNR of the acquired absorption spectra. Based on the Allan analysis performed in the present work, for 600,000 averages per sampling datum, an uncertainty of 0.01% in concentration determination is obtained for 3.49% CO_2. This uncertainty value is deduced from an absorption spectrum with an SNR of ~1620 (1σ), which corresponds to a relative uncertainty of 0.3%. It is evident that a lower SNR results in a lower measurement precision and leads to a larger measurement uncertainty.

As for fringe-like noise as shown in Fig. 5(b-2), it is usually the main factor affecting the measurement of a small change of signal in multipass cell- or cavity-enhanced absorption spectroscopy approaches. This periodic sinewave-like oscillation resulting from the Fabry–Perot etalon could be minimized by careful optical alignment. In our case, since the fringe width (~0.8 cm^{-1}) is larger than the width of absorption features as seen in Fig. 5(b-3), the etalon effect on the gas concentration determination is not a dominant factor, it was normalized out by a polynomial function fitted to the baseline (as shown in Figs. 6 and 7). The precision of the Voigt fitting algorithm, affected by the SNR, is mainly limited by Flicker noise. This $1/f$ type noise, inversely proportional to the frequency of the detected signal, can be further reduced by using a frequency modulation technique.

A 3-σ limited minimum detectable absorption coefficient of about $\sim 10^{-7}\,cm^{-1}/Hz^{1/2}$ was achieved with 600,000 averages per sampling datum. The corresponding integration time per datum was 500 ms with a sampling rate of 1.2 MS/s. In the present work, the integration time per datum was fixed at 500 ms in order to achieve maximum detection sensitivity. In this case, the corresponding measurement time required for scanning one absorption line was about 1 min.

3.4. Analysis of multiple species

In the wavelength region of 1500–1640 nm, accessible to the developed instrument, there are numerous molecular species that exhibit ro-vibrational absorptions of overtone and combination bands, which allow trace gas detection by absorption spectroscopy. Table 1 lists some of them based on the HITRAN database [23]. The minimum detectable concentration is estimated for the case using a 100-m long absorption cell at a pressure fixed at 100 Torr. In fact, other species could in principle be detected by our instrument, but

Table 1
Detectable chemical gaseous species using the developed laser-based analytical instrument

Molecules	v (cm^{-1})	λ (nm)	S (cm/molecule)	MDC (ppm)
OH	6663.8888 (0.0005)	1500.6253	$3.08\ (0.50) \times 10^{-22}$	1.5
H_2O	6647.2177 (0.0010)	1504.3888	$1.66\ (0.13) \times 10^{-23}$	68/81*
C_2H_2	6578.5761 (0.0005)	1520.0858	$1.34\ (0.02) \times 10^{-20}$	0.07/0.05*
N_2O	6566.1070 (0.0005)	1522.9724	$2.26\ (0.09) \times 10^{-23}$	41
NH_3[33]	6528.7640	1531.6835	2.33×10^{-21}	0.25[34]
HI	6489.0262 (0.0010)	1541.0633	$2.99\ (0.45) \times 10^{-22}$	2
HCN[35]	6477.8984	1543.7105	ND	ND
CO	6388.3467 (0.0005)	1565.3502	$1.69\ (0.07) \times 10^{-23}$	39/47*
$^{12}CO_2$	6240.1045 (0.0005)	1602.5373	$1.84\ (0.07) \times 10^{-23}$	47/98*
$^{12}CO_2$	6251.7611 (0.0005)	1599.5493	$6.06\ (0.24) \times 10^{-24}$	130
$^{13}CO_2$	6251.320 (0.020)	1599.6622	$2.02\ (0.16) \times 10^{-25}$	4410
H_2S[36]	6339.8676	1577.3200	1.80×10^{-22}	5.1
HDO	6329.1383 (0.0010)	1579.9939	$7.42\ (0.59) \times 10^{-26}$	13700
CH_4	6132.3620 (0.0005)	1630.6930	$3.04\ (0.12) \times 10^{-22}$	2

Notes: Numbers in parentheses are uncertainties in one standard deviation. MDC is the estimated minimum detectable concentration (signal-to-noise ratio of 3) when using a 100-m long absorption cell at a pressure of ~100 Torr. ND, not determined. S is the line intensity at reference temperature 296 K.

*Indicates the values obtained experimentally in the present work.

HITRAN is currently limited mostly to prominent telluric atmospheric absorbers and pollutants. For specific molecules of interest, the line parameters required for trace gas detection could be determined by spectroscopic laboratory studies.

4. Spectroscopic analysis of gas emission from a wood-based combustion

Spectroscopic analysis of gas species from a wood-based combustion emission has been carried out first in laboratory for chemical species identification and line selection in terms of detection sensitivity and selectivity. Gas samples have been obtained using extractive sampling technique with the help of Silonite^{TM}-coated 6 L stainless-steel canisters (Entech Instruments Inc.). The interior surface of the stainless-steel canisters is coated with inert fused silica, which provides an environment suitable for the collection of volatile compounds in the gas phase. It is suitable for storing polar and sulfur compounds. Acceptable holding times for EPA method TO14 compounds are typically 2 weeks or more. The wood-fired boiler was located at Flimwell (East Sussex, UK) and provides heating and hot water for East Sussex County Council's Woodland Enterprise Scheme building. Gas sample in the flue of the wood-fired boiler has been obtained for two different operating conditions at different temperatures: one was at $T\sim110\,^{\circ}C$ (full burn regime, denoted as regime 1), and the other at $T\sim70\,^{\circ}C$ (slumber regime, denoted as regime 2). Timely analyses were undertaken after sampling. Based on the absorption spectra of the combustion emission, four gaseous species have been identified and quantified, and the isotopic ratio of $^{13}CO_2/^{12}CO_2$ has been measured as well.

Fig. 5(a) displays FT-IR-like laser absorption spectra of gas emission when the boiler operated at full burn regime ($T\sim110\,^{\circ}C$). The spectra were recorded with a frequency tuning resolution of 10^{-3} nm. The gas pressure in the multipass cell was controlled at about 100 Torr. This value was taken as a trade-off choice between higher line absorption intensity for sensitive detection and better spectral discrimination from lines overlapping. The relevant factors involved in the selection of a specific absorption line for precise concentration measurements include the choice of a strong spectral line for high sensitivity that at the same time should be isolated from interfering lines that result from other gas species or from the same species.

Based on the available spectral data provided by the HITRAN database, simulation spectra of CO_2, CO, H_2O, C_2H_2, CH_4 and N_2O have been made for the spectral region of 1500–1640 nm with an optical path of 100 m at a pressure of 100 Torr and at 296 K. The concentrations used for the simulation were chosen such that they approached the experimental values. The spectral regions used for identification and quantification of $^{12}CO_2$, $^{13}CO_2$, H_2O, C_2H_2 and CO are given in Fig. 5(b).

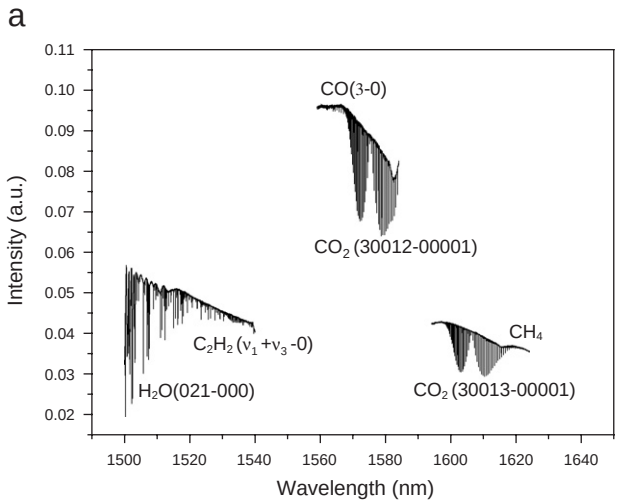

Fig. 5. (a) FT-IR-like laser absorption spectra recorded with the developed laser instrument for spectroscopic analysis of gas emission from a wood-fired burner (in full burn regime), where the pressure in the multipass cell was controlled at about 100 Torr and the frequency scan resolution was 10^{-3} nm. (b) Identification of multiple species using HITRAN-based simulation spectra.

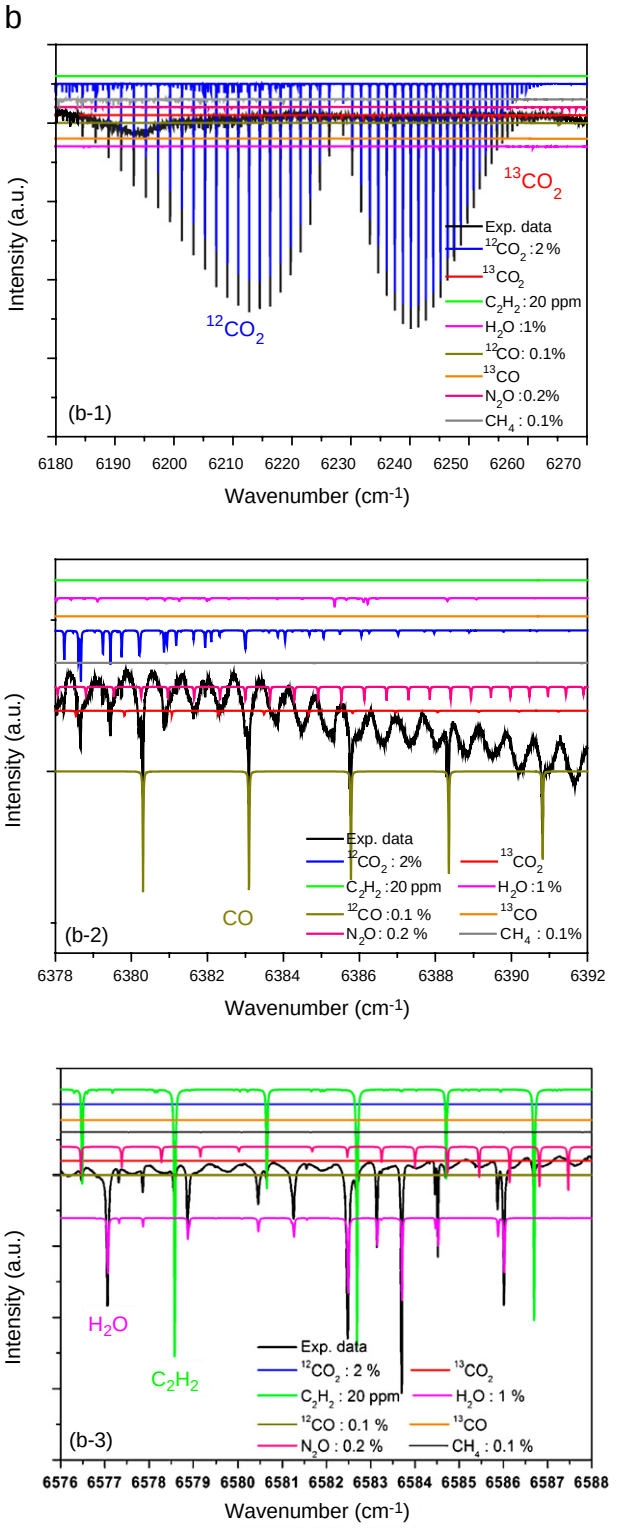

Fig. 5. (*Continued*)

All simulation spectra were shifted up or down vertically for clarity and compared with the experimental data for gas species identification and line selection. Survey spectra of 2% CO_2 for CO_2 concentration and carbon isotope ratio measurements are given in Fig. 5(b-1) for the spectral region of 6180–6270 cm^{-1}, where the P- and R-branch of the (30013-00001) band of $^{12}CO_2$ (blue curve) as well as the P- and R-branch of the (30012-00001) band of $^{13}CO_2$ (red curve) are exhibited. Fig. 5(b-2) presents calculated survey spectra of 0.1% CO (dark yellow) in the window of 6379–6392 cm^{-1}. The R(58) CO line of the (3-0) band near 6388.35 cm^{-1} was chosen for CO concentration measurement such that the spectral interference from CO_2 (blue line) and water vapor (pink line) could be minimized. Survey spectra of 1% H_2O (pink line) and 20 ppm C_2H_2 (olive line) are shown in Fig. 5(b-3) for the frequency region of 6576-6588 cm^{-1}, where the presence of the (021-000) band of H_2O and the v_1+v_3-0 band of C_2H_2 offer an opportunity of simultaneously detecting two chemical species in a limited spectral scan.

In situ measurements have been carried out by deploying the laser instrument on site. Gas emission was directly introduced from the chimney into the optical absorption cell using a two-stage diaphragm pump via a transfer line heated at ~100 °C. The inlet of the transfer line was equipped with an inline filter to protect the optical cell from particulates having diameters of 0.5 μm and above. The gas pressure was maintained at a value of 120 Torr. The temperature of the sample in the optical cell was controlled at ~100 °C within ±0.1 °C in order to avoid water vapor condensation in the cell and to minimize the temperature-dependent measurement uncertainty.

Based on the experimentally estimated noise level in the *in situ* measured CO_2 absorption spectrum, the $3-\sigma$ limited minimum detectable absorption coefficient was found to be about 2×10^{-7} $cm^{-1}/Hz^{1/2}$ that was comparable to the value of $\sim10^{-7}$ $cm^{-1}/Hz^{1/2}$ obtained under the laboratory condition. The instrument sensitivity as well as the SNR-dependent measurement precision was thus not significantly deteriorated by the field condition.

4.1. Identification and quantitative analysis of the emission gas

Line parameters, such as line intensities and line positions, were taken from the HITRAN database [23] for spectroscopic identification and gas concentration determination. Eq. (4) was used for the correction of temperature-dependent line intensity. By integrating absorbance, retrieval of emission gas concentration was made using Eq. (3). The results, determined for two different operation regimes, are listed in Table 2. Fig. 6 shows the results of spectroscopy-based gas concentration measurements.

4.2. Isotopic composition analysis

Isotope analysis of $^{13}CO_2/^{12}CO_2$ from the gas emission has been performed in the present work. Stable isotope ratio is typically expressed in parts per thousand (or per mil, ‰) relative to the Pee Dee Belemnite

Table 2
Results of gas concentration measurements and the $^{13}CO_2/^{12}CO_2$ isotope ratio determination

Molecules	v (cm^{-1})	S (cm/molecule)	Regime 1 ($T>110$ °C)	Regime 2 ($T<70$ °C)
C_2H_2	6578.5761 (0.0005)	$1.34\ (0.02)\times10^{-20}$	(6.42±0.15) ppm	(3.49±0.04) ppm
CO	6388.3467 (0.0005)	$1.69\ (0.07)\times10^{-23}$	ND[a]	(1052.5±15.3) ppm
H_2O	6583.7030 (0.0010)	$5.73\ (0.46)\times10^{-24}$	(3.59±0.24)%	(3.81±0.03)%
CO_2	6240.1045 (0.0005)	$1.84\ (0.07)\times10^{-23}$	(4.43±0.03)%	(3.49±0.01)%
$^{13}CO_2/^{12}CO_2$	6251. 320 (0.020)	$2.02\ (0.16)\times10^{-25}$	(1.1011±0.0040) %	(1.1011±0.0036) %
	6251. 7611 (0.0005)	$6.06\ (0.24)\times10^{-24}$		
Combustion efficiency[b]			~100%	~97%

Notes: Numbers in parentheses are uncertainties in one standard deviation.
[a]ND, not determined.
[b]Combustion efficiency is defined as $CO_2/(CO_2+CO)$ [37].

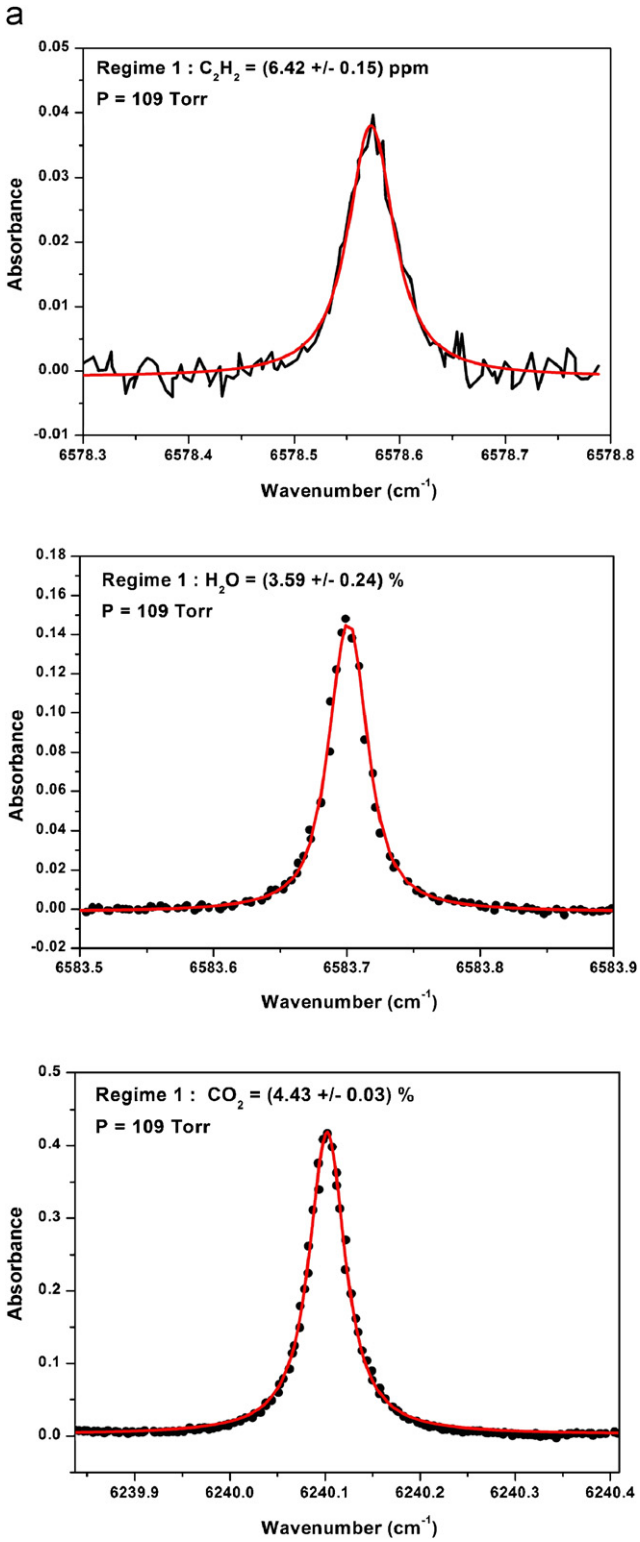

Fig. 6. Spectroscopy-based gas concentration determination for two different operation modes: (a) absorption spectra of C_2H_2, H_2O and CO_2 in full burn mode (regime 1); (b) spectra of C_2H_2, H_2O, CO_2 and CO in slumber mode (regime 2).

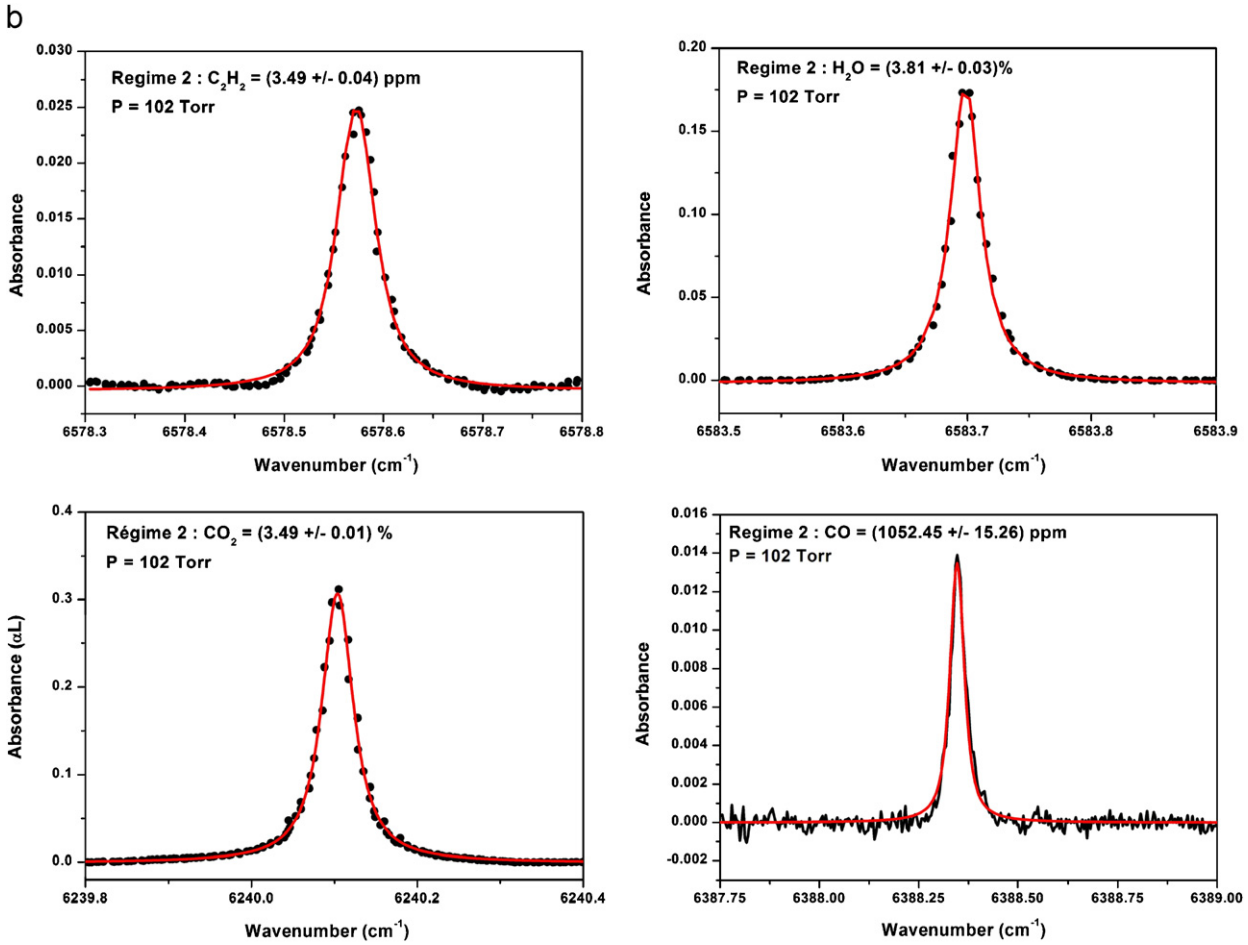

Fig. 6. (*Continued*)

(PDB) standard, the so-called δ-value. For carbon isotope ratio, we have

$$\delta^{13}\mathrm{C} = \frac{R_{\mathrm{sample}} - R_{\mathrm{PDB}}}{R_{\mathrm{PDB}}} \times 1000, \tag{5}$$

where $R_{\mathrm{sample}} = {}^{13}\mathrm{CO_2}/{}^{12}\mathrm{CO_2}$ and $R_{\mathrm{PDB}} = 0.0112372 \pm 0.0000600$, the ratio of $^{13}\mathrm{C}/^{12}\mathrm{C}$ in the $\mathrm{CO_2}$ gas sample and in the reference standard, respectively.

The isotope ratio can be determined with the ratio of the integrated area and the absorption intensities of the major and minor isotopic components:

$$R_{\mathrm{sample}} = \frac{{}^{13}A_{\mathrm{I}} \times {}^{13}n \times {}^{12}S}{{}^{12}A_{\mathrm{I}} \times {}^{12}n \times {}^{13}S}, \tag{6}$$

where A_{I} is the integrated absorbance (area under the absorption line profile) and n is the isotope abundance from the HITRAN database: ${}^{12}n = 0.9842$ and ${}^{13}n = 0.01106$.

In general, absorption line pairs of $^{13}\mathrm{CO_2}$ and $^{12}\mathrm{CO_2}$, from both the major and minor isotopic components, suitable for isotopic ratio measurement by absorption spectroscopy should meet the following criteria: having similar absorption depths at natural abundance with as large an absorption intensity as possible (for high sensitivity and high precision measurements), free of interference from other species and/or from themselves (high selectivity consideration), having similar lower state energy levels so that the effects of the

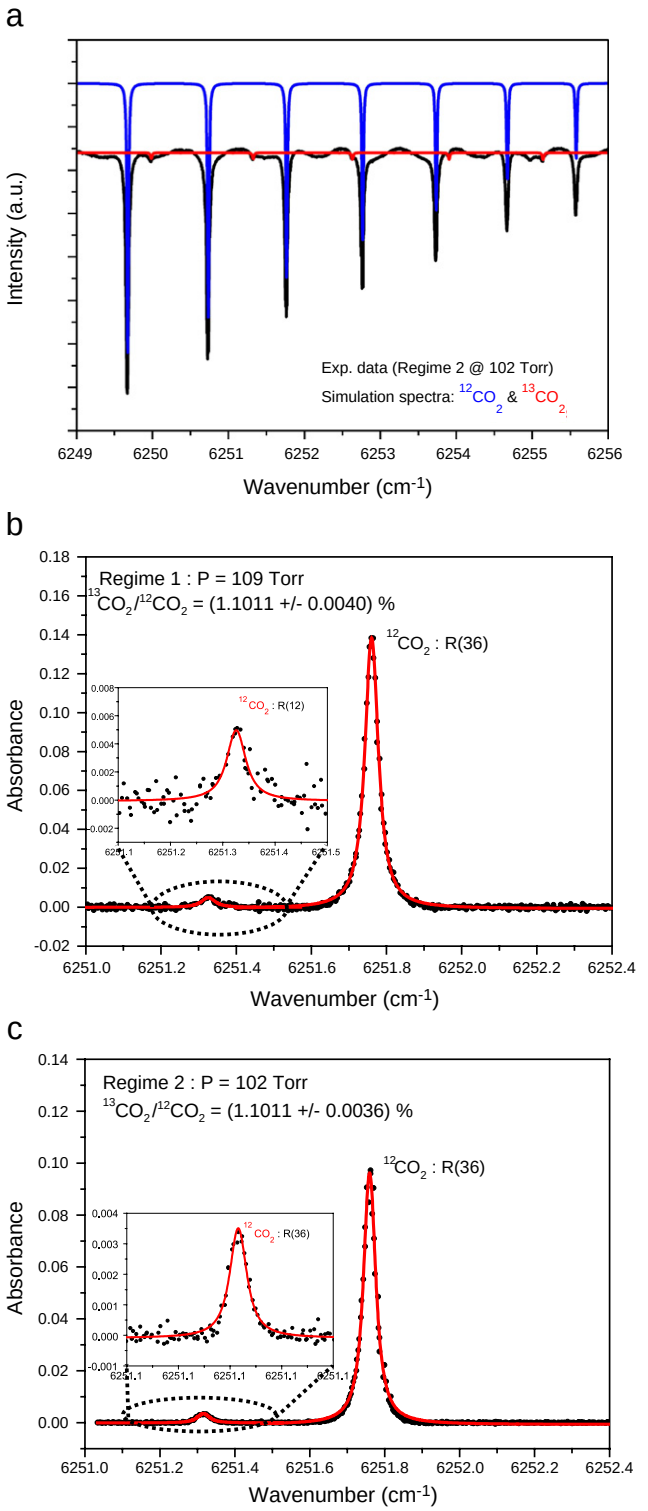

Fig. 7. (a) Experimental absorption spectra of $^{13}CO_2$ and $^{12}CO_2$ from canisters, compared with the HITRAN database simulation of 4% CO_2 with natural isotopic abundance: $^{12}n = 0.984204$ for $^{12}CO_2$ and $^{13}n = 1.10574\,10^{-2}$ for $^{13}CO_2$ at $P = 100$ Torr and $T = 296$ K. (b) and (c): $^{13}CO_2/^{12}CO_2$ isotopic ratio measurements based on laboratory analysis of combustion gas samples for regime 1 and regime 2, respectively.

temperature-dependent line intensities can be negligible. The accuracy and precision of the isotopic ratio measurement by absorption spectroscopy is mainly limited by the following factors:

(1) *Accuracy of the used line intensities*: The uncertainty in the line intensity given in the common database is in the range of $<5\%$ for $^{12}CO_2$ and 5–10% for $^{13}CO_2$ reported in HITRAN04. It is usually the main factor that limits the accuracy of the concentration determination (Eq. (3)) or δ-value measurements (Eq. (6)).
(2) As the isotopic ratio is directly deduced from the integrated area, Eq. (6), the measurement precision of the δ-value is dominated by $\Delta A_I/A_I$ that is mainly determined by the SNR of the acquired absorption spectra.
(3) *Difference of ground state energies of the used transition lines*: This factor affects to great extent the accuracy of the measurement. Temperature drifts in the sample gas cause systematic deviations in the ^{13}C quantification as given as below [29]:

$$\Delta\delta \approx \frac{\Delta E}{kT^2}\Delta T \times 1000, \tag{7}$$

where k is the Boltzmann constant, T the absolute temperature, ΔE the difference of ground-state energy. In our experiment, the temperature-dependent measurement uncertainty $\Delta\delta^{13}C$ is estimated to be 0.77‰ for $\Delta E = 458.6\,cm^{-1}$ at $T = 293\,K$ when the temperature is controlled within 0.1 K.

In the present work, the $^{12}CO_2$ R(36) and the $^{13}CO_2$ R(12) transitions of the $3\nu_1+\nu_3$ band, respectively, at 6251.7611 and 6251.3202 cm^{-1}, have been selected for the determination of the $^{13}C/^{12}C$ isotope ratio. The line intensity ratio $S(^{12}CO_2)/S(^{13}CO_2)$ for this line pair is ~30 at 296 K with $\Delta E = 458.6\,cm^{-1}$. It is worth noting that it could be also possible to select the pairs of $^{12}CO_2$ R(41) and $^{13}CO_2$ P(22) lines or $^{12}CO_2$ R(37) and $^{13}CO_2$ P(24) lines having similar intensities in order to limit the nonlinear effects on measurement precision, due to the intrinsic nonlinearity of the Beer–Lambert law and potential nonlinearity of the photodetectors. In this case, the transition lower-state energies are quite different (see Table 3) and the measurement precision suffers from the temperature variation in the gas mixture during measurements. Usually, the dual-path balanced absorption technique using different optical path lengths is employed to compensate the large abundance difference and balance the signal levels [3,6,7,30]. In the present work, a single absorption cell was used, which eliminates the dual-channel effects on the isotope measurements accuracy due to the drifts in the temperature difference between the two cells, and also the systematic deviation resulting from the pressure difference and the optical path length difference between the cells.

Spectroscopy-based measurements of the $^{13}C/^{12}C$ isotopic ratio in CO_2 have been performed in the laboratory with the help of canisters. Fig. 7 shows absorption spectra of $^{13}CO_2$ and $^{12}CO_2$ near 6521.5 cm^{-1} for regimes 1 and 2, respectively. In order to reduce the measurement uncertainty, 23 line pairs of $^{13}CO_2$ and $^{12}CO_2$ of the $3\nu_1+\nu_3$ band absorption spectrum, spanning the spectral region from 6216.8 to 6262.3 cm^{-1}, have been used for isotopic ratio determination. The used 23 line pairs have been carefully selected such that the spectral interferences with other molecular species could be minimized. It is worth noting, as uncertainties of the line intensities given in the HITRAN database vary from about 3% to 10%, that the use of 23 line pairs permits one to improve not only the measurement precision but also the measurement accuracy.

Table 3
Selection of line pairs of $^{12}CO_2$ and $^{13}CO_2$ for isotope ratio measurement. $\Delta\nu$ is the frequency separation between the two lines

ν (cm^{-1})		S (cm/molecule)		$\lvert\Delta\nu\ (cm^{-1})\rvert$	S ratio	$\lvert\Delta E\ (cm^{-1})\rvert$	$\Delta\delta^{13}C/\Delta T$ ($‰K^{-1}$)
$^{12}CO_2$	$^{13}CO_2$	$^{12}CO_2$	$^{13}CO_2$				
R(36) 6251.7611	R(12) 6251.3202	6.058×10^{-24}	2.025×10^{-25}	0.4409	29.92	458.7	8
R(41) 6222.2257	P(22) 6222.7876	1.03310^{-25}	1.762×10^{-25}	0.5619	0.59	1142.2	19
R(37) 6220.3203	P(24) 6220.8361	1.692×10^{-25}	1.607×10^{-25}	0.5158	1.05	982.3	16

S ratio is the $S(^{12}CO_2)/S(^{13}CO_2)$ ratio between the intensities for the two lines. ΔE is the difference of ground-state energies. The temperature-dependent delta value $\Delta\delta^{13}C/\Delta T$ is calculated at $T = 293\,K$.
Notes: Positions, intensities and ground-state energies are taken from the HITRAN database [23].

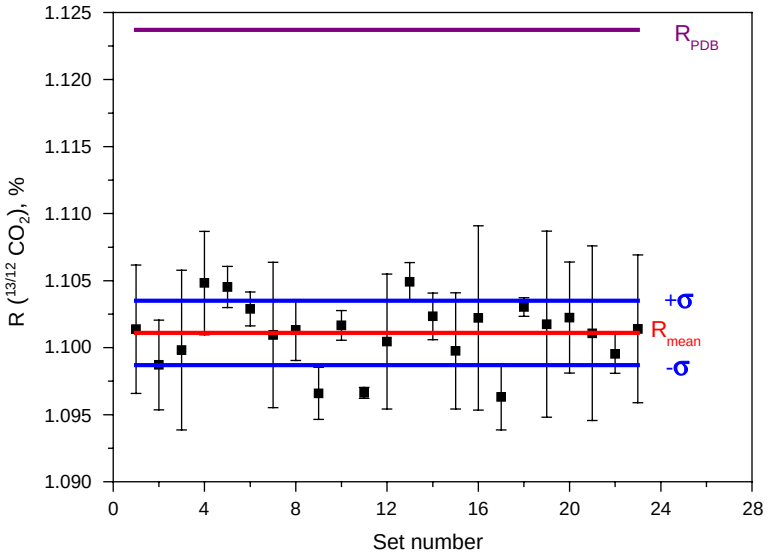

Fig. 8. Results of the $^{13}CO_2/^{12}CO_2$ isotope ratio measurements using 23 line pairs of $^{13}CO_2$ and $^{12}CO_2$ of the $3\nu_1+\nu_3$ band absorption spectra spanning the spectral region from 6216.8 to 6262.3 cm^{-1}. The error bar represents $1-\sigma$ standard deviation. The reference standard R_{PDB} is given for comparison.

The measurements have been performed for regimes 1 and 2, respectively. The mean value and the standard deviation of the averaged $^{13}CO_2/^{12}CO_2$ ratio is $(1.1011\pm0.0040)\%$ for regime 1 and $(1.1011\pm0.0036)\%$ for regime 2, respectively. The averaged value of the $^{13}CO_2/^{12}CO_2$ ratio is the same for both regimes. In fact, the natural abundances of the stable isotopes are determined during nucleosynthesis and independent of the operation regime of the boiler. The $1-\sigma$ standard deviation values are slightly different for the two combustion regimes. This may be attributed to the uncertainty in the determination of the integrated area, which is related to the SNR of the recorded absorption spectrum. In our experiments, the minimum detectable absorption coefficients, deduced from the experimentally estimated SNR, are $1.4\times10^{-7}\,cm^{-1}$ for regime 1 and $2.3\times10^{-8}\,cm^{-1}$ for regime 2, respectively. Based on these measurements, an averaged value of $(1.1011\pm0.0024)\%$ for the $^{13}CO_2/^{12}CO_2$ ratio has been determined, as shown in Fig. 8. The corresponding δ-value relative to PDB standard has been found to be $(-20.17\pm2.14)‰$. The value of $1-\sigma$ standard deviation includes both systematic and random (statistical) errors. The relatively low precision of $\Delta\delta^{13}C$ is mainly caused by the uncertainty in the integrated absorbance measurements. For instance, the relative precision of $\Delta A_I/A_I$ used for the isotope ratio determination is typically 0.6% for $^{12}CO_2$ and 20% for $^{13}CO_2$. Although the reported precision of $\Delta\delta^{13}C$ is comparable to the value of 3.7‰ recently reported by Kasyutich et al. [10] for the $^{13}C/^{12}C$ ratio measurements in 5% CO_2 in human breath sample, further improvement in measurement sensitivity could allow reduction in uncertainty of the determined integrated area, in particular for $^{13}CO_2$. For this purpose, the balance absorption spectroscopic technique [3,6,7,30] would be suitable to balance the absorption levels of $^{12}CO_2$ and $^{13}CO_2$ so that they have similar absorption depths at natural abundance.

It is worth noting that the typical $\delta^{13}C$ value for wood is $(-25\pm2)‰$ [31] and it may vary significantly with the type and age of wood. Schultze et al. [32] reported in a recent work an average value between -27 and $-22‰$ for pine trees over a 22-year period. The $\delta^{13}C$ value of $-20.17‰$ obtained in the present work is in good agreement with the typical value for wood.

5. Conclusions

A compact and field deployable laser instrument has been applied for the analysis of a wood-based combustion emission. Chemical species of C_2H_2, CO, CO_2 and H_2O in combustion emission have been

identified and quantified using direct absorption spectroscopy. Based on integrated absorbance measurements, the $^{13}C/^{12}C$ isotope abundance ratio in carbon dioxide from the combustion emission has been determined without any sample preconcentration and purification, which are usually required for mass spectrometric analysis. The averaged value of the $^{13}CO_2/^{12}CO_2$ ratio is found to be $(1.1011 \pm 0.0024)\%$. Although the corresponding δ-value of $-20.17‰$, relative to PDB standard, is in good agreement with the typical value for wood within the estimated $\pm 2.14‰$ measurement uncertainty and we believe that the discrepancy between the measured $\delta^{13}C$ and the typical value is due to the variety of wood, investigation in measurement accuracy would be addressed in the future with the help of a standard reference. Further improvement in measurement sensitivity and precision could be made by implementing the frequency modulation technique to multipass direct absorption spectroscopy or using cavity-enhanced absorption spectroscopy in conjunction with dual-path balanced absorption technique in order to meet a precision of $<1‰$ for real-world applications in various areas, e.g. atmospheric chemistry, ecology, geochemistry and medical diagnoses.

Acknowledgments

This work was supported in part by the INTERREG European program (EDER French Grant No111/118), the ACI national program (CNRS-DGA/NMAC/10), the IRENI regional program and the BQR program of the Université du Littoral Côte d'Opale. We are grateful to A. Mercier (CCM) for valuable technical assistance. We are also grateful to the reviewers for their helpful and constructive comments.

References

[1] Becker J, Sauke T, Loewenstein M. Stable isotope analysis using tunable diode laser spectroscopy. Appl Opt 1992;31:1921–7.
[2] Murnick D, Peer B. Laser-based analysis of carbon isotope ratios. Science 1994;263:945–7.
[3] Erdélyi M, Richter D, Tittel F. $^{13}CO_2/^{12}CO_2$ isotopic ratio measurements using a difference frequency-based sensor operating at 4.35 μm. Appl Phys B 2002;75:289–95.
[4] Gagliardi G, Castrillo A, Iannone R, Kerstel E, Gianfrani L. High-precision determination of the $^{13}CO_2/^{12}CO_2$ isotope ratio using a portable 2.008 μm diode-laser spectrometer. Appl Phys B 2003;77:119–24.
[5] Castrillo A, Casa G, Kerstel E, Gianfrani L. Diode laser absorption spectrometry for $^{13}CO_2/^{12}CO_2$ isotope ratio analysis: investigation on precision and accuracy levels. Appl Phys B 2005;81:863–9.
[6] Weidmann D, Wysocki G, Oppenheimer C, Tittel F. Development of a compact quantum cascade laser spectrometer for field measurements of CO_2 isotopes. Appl Phys B 2005;80:255–60.
[7] McManus J, Zahniser M, Nelson D, Williams L, Kolb C. Infrared laser spectrometer with balanced absorption for measurement of isotopic ratios of carbon gases. Spectrochim Acta A 2002;58:2465–79.
[8] Castrillo A, Casa G, Van Burgel M, Tedesco D, Gianfrani L. First field determination of the $^{13}C/^{12}C$ isotope ratio in volcanic CO_2 by diode-laser spectrometry. Opt Express 2004;12:6515–23.
[9] Crosson E, Ricci K, Richman B, Chilese F, Owano T, Provencal R, et al. Stable isotope ratios using cavity ring-down spectroscopy: determination of $^{13}C/^{12}C$ for carbon dioxide in human breath. Anal Chem 2002;74:2003–7.
[10] Kasyutich V, Martin P, Holdsworth R. An off-axis cavity-enhanced absorption spectrometer at 1605 nm for the $^{12}CO_2/^{13}CO_2$ measurement. Appl Phys B 2006;85:413–20.
[11] Sonnenfroh D, Allen M. Absorption measurements of the second overtone band of NO in ambient and combustion gases with a 1.8-μm room-temperature diode laser. Appl Opt 1997;36:7970–7.
[12] Mihalcea R, Baer D, Hanson R. Diode laser sensor for measurements of CO, CO_2 and CH_4 in combustion flows. Appl Opt 1997;36:8745–52.
[13] Upschulte B, Sonnenfroh D, Allen M. Measurements of CO, CO_2, OH and H_2O in room-temperature and combustion gases by use of a broadly current-tuned multisection InGaAsP diode laser. Appl Opt 1999;38:1506–12.
[14] Aizawa T, Kamimoto T, Tamaru T. Measurements of OH radical concentration in combustion environments by wavelength-modulation spectroscopy with a 1.55-μm distributed-feedback diode laser. Appl Opt 1999;38:1733–41.
[15] Wang J, Maiorov M, Baer D, Garbuzov D, Connolly J, Hanson R. In situ combustion measurements of CO with diode-laser absorption near 2.3 μm. Appl Opt 2000;39:5579–89.
[16] Webber M, Kim S, Sanders S, Baer D, Hanson R, Ikeda Y. In situ combustion measurements of CO_2 by use of a distributed-feedback diode-laser sensor near 2.0 μm. Appl Opt 2001;40:821–8.
[17] Nikkari J, Di Iorio J, Thomson M. In situ combustion measurements of CO, H_2O and temperature with a 1.58-μm diode laser and two-tone frequency modulation. Appl Opt 2002;41:446–52.
[18] Teichert H, Fernholz T, Ebert V. Simultaneous in situ measurement of CO, H_2O and gas temperatures in a full-sized coal-fired power plant by near-infrared diode lasers. Appl Opt 2003;42:2043–51.

[19] Jennings D. Absolute line strengths in v_4, $^{12}CH_4$: a dual-beam diode laser spectrometer with sweep integration. Appl Opt 1980;19: 2695–700.
[20] Cousin J, Masselin P, Chen W, Boucher D, Kassi S, Romanini D, et al. Application of a continuous-wave tunable erbium doped fiber laser to molecular spectroscopy in the near infrared. Appl Phys B 2006;83:261–6.
[21] Macko P, Romanini D, Mikhailenko S, Naumenko O, Kassi S, Jenouvrier A, et al. High sensitivity CW-cavity ring down spectroscopy of water in the region of the 1.5 μm atmospheric window. J Mol Spectrosc 2004;227:90–108.
[22] Sauke TB, Becker JF. Modeling, measuring, and minimizing the instrument response function of a tunable diode laser spectrometer. JQSRT 2005;91:453–84.
[23] Rothman LS, Jacquemart D, Barbe A, Benner D, Birk M, Brown LR, et al. The HITRAN 2004 molecular spectroscopic database. JQSRT 2005;96:139–204.
[24] Gamache RR, Hawkins RL, Rothman LS. Total internal partition sums in the temperature range 70-3000 K: atmospheric linear molecules. J Mol Spectrosc 1990;142:205–19.
[25] Toth RA. Extensive measurements of $H_2^{16}O$ line frequencies and strengths: 5750–7695 cm^{-1}. Appl Opt 1994;33:4851–67.
[26] Werle P, Mucke R, Slemr F. Limits of signal averaging in atmospheric trace gas monitoring by tunable diode laser absorption spectroscopy. Appl Phys B 1993;57:131–9.
[27] Werle P, Mazzinghi P, Amato F, De Rosa M, Maurer K, Slemer F. Signal processing and calibration procedures for in situ diode-laser absorption spectroscopy. Spectrochim Acta A 2004;60:1685–705.
[28] Weibring P, Richter D, Fried A, Walega JG, Dyroff C. Ultra-high-precision mid-IR spectrometer II: system description and spectroscopic performance. Appl Phys B 2006;85:207–18.
[29] Schupp M. Entwicklung und demonstration einer laser-spektroskopischen methode zur messung des Kohlenstoffisoto-penverhältnisses in methan. PhD dissertation, Universität Mainz, Mainz, Germany, 1992.
[30] Uehara K, Yamamoto K, Kikugawa T, Yoshida N. Isotope analysis of environmental substances by a new laser-spectroscopic method utilizing different pathlengths. Sensors Actuators B 2001;74:173–8.
[31] Stuiver M, Polach H. Discussion: reporting of ^{14}C data. Radiocarbon 1977;19:355–63.
[32] Schulze B, Wirth C, Linke P, Brand WA, Kuhlmann I, Horna V, et al. Laser ablation-combustion-GC-IRMS—a new method for online analysis of intra-annual variation of $\delta^{13}C$ in tree rings. Tree Physiol 2004;24:1193–201.
[33] Lundsberg-Nielsen L, Hegelund F, Nicolaisen F. Analysis of the high-resolution spectrum of ammonia in the near-infrared region, 6400–6900 cm^{-1}. J Mol Spectrosc 1993;162:230–45.
[34] Claps R, Englich F, Leleux D, Richter D, Tittel F, Curl R. Ammonia detection by use of near-infrared diode-laser-based overtone spectroscopy. Appl Opt 2001;40:4387–94.
[35] Sasada H, Yamada K. Calibration lines of HCN in the 1.5-μm region. Appl Opt 1990;29:3535–47.
[36] Modugno G, Corsi C, Gabrysch M, Inguscio M. Detection of H_2S at the ppm level using a telecommunication diode laser. Optics Comm 1998;145:76–80.
[37] Olsson M, Kjällstrand J. Low emissions from wood burning in an ecolabelled residential boiler. Atmos Environ 2006;40:1148–58.